UNCLASSIFIED

AD 297 438

UNCLASSIFIED

63-2-5

297 438

U. S.   A R M Y
TRANSPORTATION RESEARCH COMMAND
FORT EUSTIS, VIRGINIA

TCREC TECHNICAL REPORT 62-82

RESEARCH ON THE VOLUME RECOMBINATION
OF CESIUM IONS

Task 9R99-20-001-08

Contract DA 44-177-TC-694

November 1962

prepared by:

RADIO CORPORATION OF AMERICA
RCA Laboratories
Princeton, New Jersey

ASTIA

MAR 1 1963

TISIA   0

DISCLAIMER NOTICE

The report has been reviewed and has been found to be technically sound.

Conclusions and recommendations contained in the report are concurred in by this command.

FOR THE COMMANDER:

KENNETH B. ABEL
Captain,   TC
Adjutant

APPROVED BY:

JAMES P. WALLER
USATRECOM Project Engineer

INTERIM ENGINEERING REPORT NO. 1

For the Period

October 1, 1960 – March 31, 1962

Report Issue Date – October 15, 1962

RESEARCH ON THE VOLUME RECOMBINATION OF

CESIUM IONS

Prepared by:

**RADIO CORPORATION OF AMERICA
RCA LABORATORIES
PRINCETON, NEW JERSEY**

Report Prepared by: P. V. Goedertier
J. M. Hammer *(Project Engineer)*

Prepared for:

**U. S. ARMY TRANSPORTATION RESEARCH COMMAND
TRANSPORTATION CORPS
FORT EUSTIS, VIRGINIA**

TABLE OF CONTENTS

INTRODUCTION

Interest in plasma physics has been greatly increased by the practical uses that are envisaged for plasmas in such devices as thermionic energy converters, plasma propulsion engines, and thermonuclear reactors. At the high plasma densities required for realisitic devices, one of the more important deionizing mechanisms tending to destroy the plasma is radiative recombination. Hence, knowledge of the value of the radiative recombination coefficient or cross-section is essential to the rational design of a large class of useful devices. Up to the present time consistent and accurate values of the radiative recombination cross-section have not been available. As a result several measurements of recombination are in progress in various laboratories. Among these is the present program being supported at RCA Laboratories by the U. S. Army Transportation Research Command. This program is distinguished by utilizing a beam method ultimately capable of separating the components of the reaction before and after recombination takes place. This technique is not subject to the uncertainties which plague the other methods, all of which rely on measurements made on a complex plasma.

Measurements of the volume recombination coefficient, a, of ions and electrons in gas discharge afterglows using photometric and probe techniques were made by various workers during the late 1920's and 1930's.[1-7] These measurements yielded values of a of the order of 10^{-10} cm^3/sec. Later, microwave measurements of the complex conductivities of afterglows were used to find the ambipolar diffusion coefficient and the volume recombination coefficient.[8-15] These later measurements yielded values of the recombination coefficient which were about three orders of magnitude larger than those found by the probe method. Theoretical calculations of radiative and dielectronic recombination[16-18] predict values of a some two orders of magnitude ($a = 10^{-12} - 10^{-13}$) smaller than the values found by the probe method and, hence, five orders of magnitude smaller than the values yielded by microwave measurements. However, the theoretical values of the dissociative recombination coefficient[19,20] are of the same order of magnitude (10^{-7}) as those found by the microwave measurements. On the basis of the low degree of ionization ($10^{-4} - 10^{-3}$ per cent) employed in the microwave measurements as compared to the probe measurements ($10^{-2} - 10^{-1}$ per cent), it has been supposed that the microwave experiments measure dissociative recombination rather than radiative recombination.[13,21] There seems to be no good guess as to just what was measured by the probe experiments.

More recently D'Angelo has proposed that a three-body type of recombination involving two electrons and one ion can explain the comparitively large values of a that have been observed.[22] Thus, at high electron densities ($10^{12} - 10^{13}$ cm^3) he predicts a's to be from 20-70 times the usual (theoretical) radiative recombination coefficient for hydrogen. That this type of three-body recombination is important in dense helium plasmas is confirmed in an experiment by Kuckes et al.[23] Hinnov and Hirschberg, in a different calculation involving a two-electron, one-ion type of recombination, predict even higher values of a at high electron densities. They also measure the recombination coefficient in plasma afterglows (helium and hydrogen) by spectroscopic means and get good agreement with their computation.[24] In addition, Hinnov and Hirschberg's computation is in substantial agreement with the computation of Bates and Kingston[25] and that of McWorter.[26] Finally, in a very recent paper Byron et al[27] give a "simple general method of calculating both the electron temperature and the net rate of three-body recombination." Their calculation is in good agreement with that of Bates and Kingston.

1

Insofar as specific measurements on the cesium recombination are concerned, the only reasonable ones to date appear to be those made by Mohler using the probe technique.[26] He finds $a = 3.4 \times 10^{-10}$ cm^3/sec.

It is clear that further work on recombination is necessary to resolve the discrepancies that still exist despite some encouraging recent work. The microwave and probe techniques suffer the common disability of not being able to distinguish clearly between the particular types of recombination taking place. In addition, the probe experiments are subject to all the errors inherent in the use of Langmuir probes to measure plasma properties, as has been shown by work performed at these Laboratories.[28] All the experimental methods that have been employed involve the determination of the recombination coefficient. These experiments are thus always performed on a complex plasma in which it is difficult to isolate the specific interaction.

To help resolve these difficulties and to supplement the very scant information now available on cesium recombination, the present experiment to measure the cross-section rather than the coefficient for the volume recombination of cesium ions and electrons has been undertaken.

The method employed here to measure recombination is one that has not heretofore been used for this purpose. This method, in brief, involves the passage of a beam of ions, which potentially may be mass analyzed, through a modulated "cloud" of electrons. The emergent beam is then passed through a transverse electric field which separates ions from atoms. The modulated current of recombined atoms is detected by means of the secondary electrons emitted when the relatively fast atoms fall on a metallic surface. One is thus able to find the cross-section for recombination between electrons and ions in an unambiguous way.

In the following sections, the beam technique of measuring radiative recombination will be described and analyzed. First the general experimental technique will be outlined. In order to do this, a brief review of the theoretical analysis of the passage of an ion beam through an electron cloud will be given. An overall picture of the apparatus will then be drawn and the general method of operation explained. Following this, each component of the apparatus will be described in modest detail. The results of tests made on the individual components will be included where pertinent. At the conclusion, a brief description of some very preliminary tests that have been made on the apparatus will be given. The results of these tests, which give some indication that the method is workable, will be discussed in conjunction with an overall critique on the sensitivity of the method.

2

BASIC OF THE ION BEAM METHOD
OF MEASURING RECOMBINATION

In order to understand how the beam method of measuring recombination works, consider the following analysis of the passage of an ion beam of current at any point I_i and of homogeneous velocity v_i through an electron cloud which has a density of electrons N_o. If for the moment the electrons are considered as being at rest but randomly distributed in space, then the current of ions dI_i which is lost from the ion beam by recombination after the ion beam has traveled a distance dx through the electron cloud is

$$dI_i = - I_i N_o Q_R (v_r) dx. \tag{1}$$

Here $Q_R (v_r)$ is the cross-section for recombination at a relative velocity between the ion and the electrons of v_r. Integrating (1), the current of ions (I_i) remaining after the ion beam travels a distance x through the electron cloud is found to be

$$I_i = I_o e^{-N_o Q_R(v_r) x}.$$

I_o is the initial ion current which enters the electron cloud at x = o. The current of atoms I_R (recombined ions) at the point x will be given by the difference $I_o - I_i$; thus

$$I_R = I_o (1 - e^{-N_o Q_R(v_r) x}).$$

In any practical case $N_o Q_R (v_r) x << 1$ (being approximately 10^{-10}); hence, to a high degree of accuracy,

$$I_i = I_o (1 - N_o Q_R (v_r) x) \tag{2a}$$

and

$$I_R = I_o N_o Q_R (v_r) x. \tag{2b}$$

In an actual physical situation, the electrons, rather than being stationary, will be moving with the Maxwellian velocity distribution appropriate to the temperature of the electron cloud (T_o). From the analysis of the free path of a particle of one type in a gas of another, the probability per unit time θ_{v_i, T_o} that an ion with velocity v_i makes a recombination collision with an electron is[29]

$$\theta_{v_i, T_o} = N_o \bar{Q}_R (v_i)(2kT_o/\pi m)^{\frac{1}{2}} \left[e^{-\xi^2} + (2\xi + \frac{1}{\xi}) \int_o^\xi e^{-y^2} dy \right]. \tag{3}$$

Here $\xi = v_i (m/2\,kT_o)^{1/2}$, m is the electron mass, k is Boltzmann's constant, and $\bar{Q}_R(v_i)$ is the recombination cross-section averaged over the relative velocity between ion and electrons (v_r). In deriving (3), $Q_R(v_r)$ enters into the integral. The approximation of taking $Q_R(v_r)$ out of the integrand as a constant equal to $\bar{Q}_R(v_i)$ was made. In addition, to a good degree of approximation, $\bar{Q}_R(v_i) = Q_R(\bar{v}_r)^{30}$ where $\bar{v}_r$ is the average relative velocity between electrons and ions. The ions travel a distance x in time x/v_i, and thus each ion has a probability $\theta_{v_i,T_o} x/v_i$ of making a recombination collision in traveling this distance. As a result, the current of recombined ions (atoms) is

$$I_R = I_o\, \theta_{v_i,T_o}\, x/v_i. \tag{4}$$

If an effective electron density N_e is defined as

$$N_e = \theta_{v_i,T_o}/v_i\, Q_R(\bar{v}_r), \tag{5}$$

by solving (5) for θ_{v_i,T_o} and substituting in (4) one obtains, in analogy with equations (2a, b),

$$I_R = I_o\, N_e\, Q_R(\bar{v}_r)\, x \tag{6a}$$

$$I_i = I_o\, (1 - N_e\, Q_R(\bar{v}_r)\, x). \tag{6b}$$

Equations (6a, b) form the basis of the beam method of measuring the recombination cross-section. If a beam of ions of known current is passed through an electron cloud of known density and temperature and if the current of recombined atoms can be measured, equation (6a) can be used to find $Q_R(\bar{v}_r)$.

Measurements that have been made in the past yield the recombination coefficient rather than the recombination cross-section. As a result, it is useful to give the relation between these quantities. The recombination coefficient, a, may be understood as follows. Consider a plasma with an ion density N_i and an electron density N_o. The rate of loss of ions by recombination is equal to the rate of loss of electrons and

$$\frac{dN_i}{dt} = \frac{dN_o}{dt} = -a\, N_o\, N_i. \tag{7}$$

Consider for the moment a stationary cloud of electrons and an ion beam impinging on the electrons with velocity v_i and current density J_i. The ion density is then $N_i = J_i/v_i\, e$ and $edN_i/dt = dJ_i/dx$ since v_i is considered not to vary with time or distance. Since equation (2) applies equally well to the current density for constant diameter beams which are here assumed, $dJ_i/dx = -J_o N_o Q_R(v_i)$. Thus from (7), $J_o\, Q_R(v_i) = e\, a(v_i)N_i$, where $a(v_i)$ is the recombination coefficient for a relative velocity v_i. In any practical case, $J_i \doteq J_o$ and

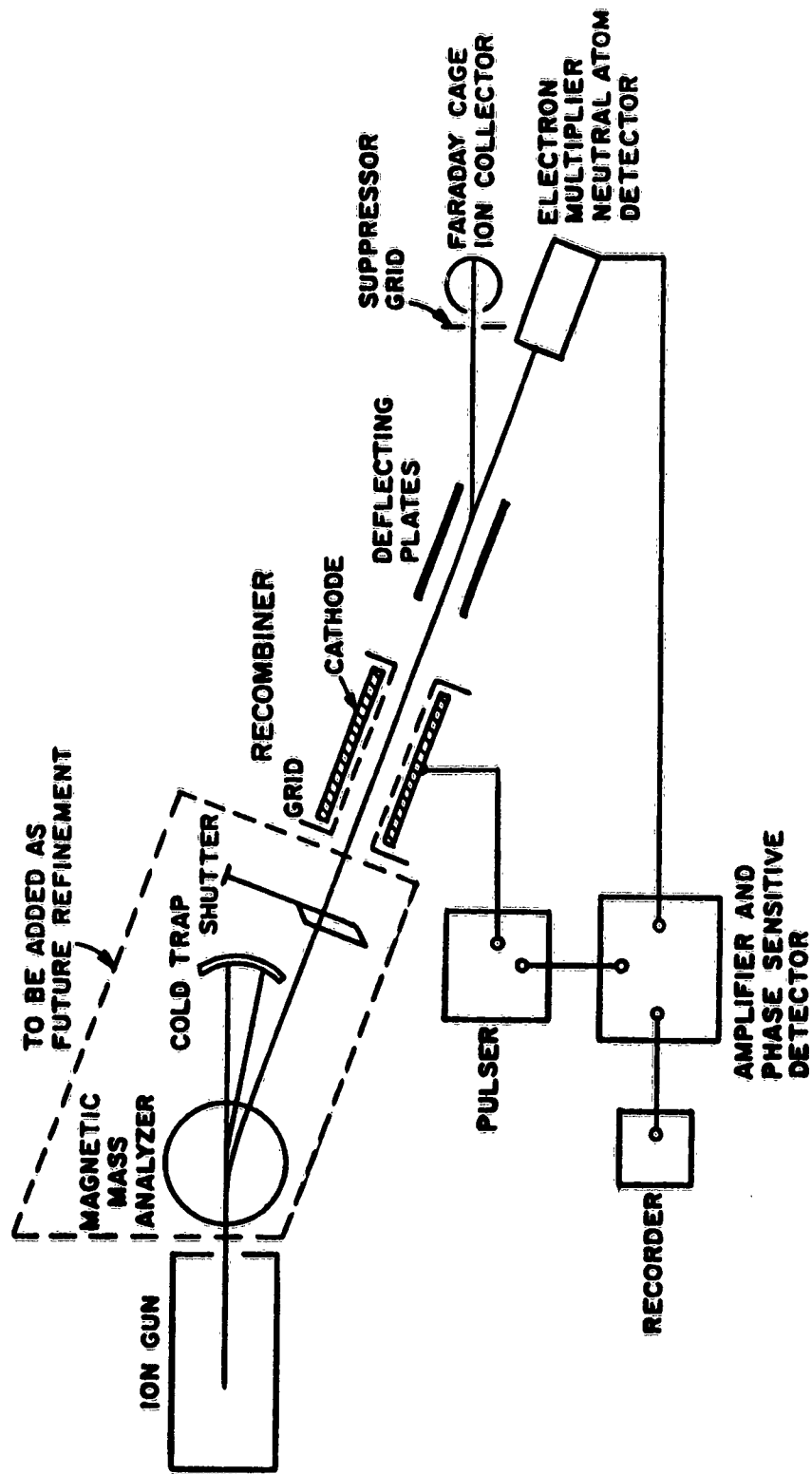$$Q_R(v_i) = \frac{a(v_i)}{v_i}. \tag{8}$$

4

In a real situation, the measured a would be an average over the relative velocity between the ions and electrons. Thus $a = \int v \, Q_R(v) \, f(v) \, dv$, where $f(v)$ is the normalized distribution of relative velocities between the electrons and ions. A good approximation[30] to this integral is
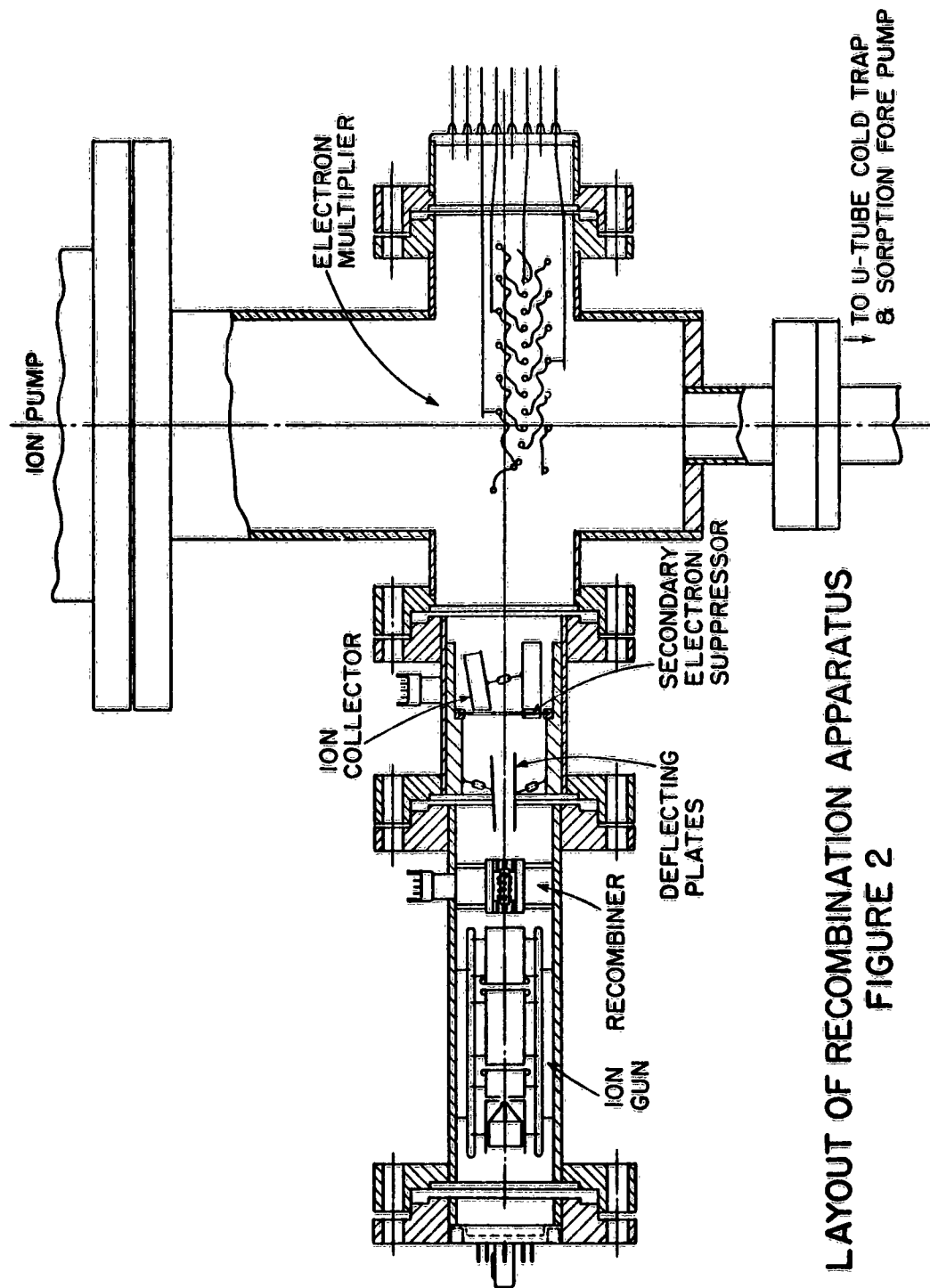
$$a \doteq \bar{v}_r \, Q_R(\bar{v}_r) . \tag{9}$$

Thus to the degree of approximation of (9), a and Q are simply related through the average relative velocity between ion and electron.

Thus, as a brief summary: if an ion beam of known current is allowed to pass through an electron cloud of known length, density, and temperature and if the current of recombined ions (atoms) can be measured, the recombination cross-section is obtained by applying equation (6a). A schematic diagram of the experimental apparatus constructed to implement the method outlined in the previous section is shown in Figure 1. The actual layout of the apparatus is shown in Figure 2. An ion beam is formed at the ion gun and focussed through the recombiner. A cloud of electrons is formed and can be modulated in the recombiner by the action of the grid. The density of electrons can be computed from knowledge of the grid current and the recombiner geometry. After passing through the electron cloud, the beam, now consisting of ions and a relatively small number of recombined ions (atoms), passes through the electric deflecting plates, where the ions are deflected upward while the atoms continue in the original direction. The ions are collected in a Faraday cup ion collector which is guarded by a secondary electron suppressing electrode. Because of the small amount of recombination that takes place, the current to the ion collector is essentially I_o. The undeflected atoms continue to the first dynode of an electron multiplier. The relatively high-energy atoms are detected by means of the secondary electrons which are emitted when the atoms fall on the dynode. The multiplier output is proportional to the recombined current of atoms. The constant of proportionality must be found by means of subsidiary calibrations which will be described later. The entire assembly is housed in a vacuum system capable of maintaining very high and clean vacuum conditions yet flexible enough to permit convenient component replacement and the addition of various interesting modifications, such as mass selection of the ions prior to recombination. Initial trials of the apparatus have been made, and signals, which it is believed are due to recombination, have been observed. The qualifications for this latter observation will be given in the discussion section. A prime requirement for the final evaluation of any measurements made in this apparatus is an understanding of the operation of each of the components. Thus, in the following sections, each of the components will be discussed in detail.

5

ION GUN

MAGNETIC
MASS
ANALYZER

TO BE ADDED AS
FUTURE REFINEMENT

COLD TRAP
SHUTTER

RECOMBINER

GRID

CATHODE

DEFLECTING
PLATES

SUPPRESSOR
GRID

FARADAY CAGE
ION COLLECTOR

ELECTRON
MULTIPLIER
NEUTRAL ATOM
DETECTOR

PULSER

AMPLIFIER AND
PHASE SENSITIVE
DETECTOR

RECORDER

APPARATUS TO MEASURE ALKALI RECOMBINATION
FIGURE I

6

ION PUMP

ELECTRON
MULTIPLIER

TO U-TUBE COLD TRAP
& SORPTION FORE PUMP

ION
COLLECTOR

SECONDARY
ELECTRON
SUPPRESSOR

DEFLECTING
PLATES

RECOMBINER

ION
GUN

LAYOUT OF RECOMBINATION APPARATUS
FIGURE 2

7

KEY

V_1 = ION SOURCE

V_2 - V_5 FOCUSING ELECTRODES
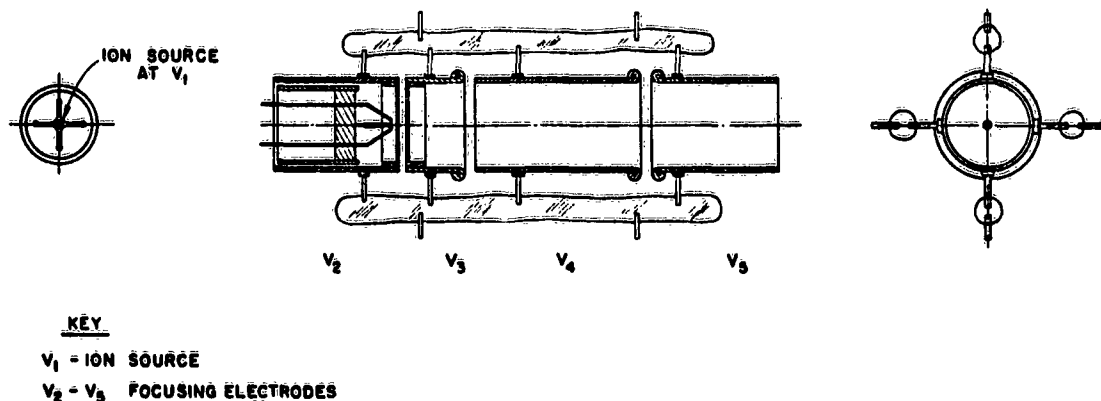
ION GUN

FIGURE 3

maximum current, will diverge by a given amount in approximately one-half the distance that one would calculate from the simple theory. Thus, the current predicted using (10) should be reduced by at least a factor of 4. Using these considerations, ion currents approximately ten times as large as those that have been obtained would be predicted. Since the ion gun design is theoretically capable of providing the proper convergence to reach the limiting current density, it is clear that the system is limited by the ion source. In addition, the nonuniform nature of the emission from the cesium aluminum silicate source causes a considerable variation of the optimum focusing voltages as the source ages. As a result, the use of a porous plug type of ion source to replace the present source is being considered.

THE RECOMBINER

In order to obtain a high density of thermal electrons in some region, it is neces-
sary to overcome the space charge force tending to keep the electrons apart. There are
two methods to do this that have been considered here and which will be discussed. One
of these methods is now being employed in the apparatus, and there is a strong likelihood
that the second method, which yields a higher density, will be put into effect in the future.
Briefly, the first method overcomes space charge by accelerating the electrons towards the
axis in a cylindrical geometry. This method gives a high electron density over a very small
volume. The second method achieves a high electron density by neutralizing the electrons
with positive ions. The possible effect of the ions on the recombination will be discussed
later. Ash and Gabor[37] have described electron interaction experiments which used both
of these methods and in which some experimental values of the electron densities were
found. They do not however, give a theoretical treatment which is appropriate to the condi-
tions of the recombination experiment.

The recombiner using the first method considered and incorporated in the recombi-
nation apparatus at the present time is shown in Figure 4. In a cylindrical arrangement,
electrons are accelerated towards the recombiner axis by a positive voltage applied to the
grid. The action of the electron space charge depresses the potential in the recombiner to
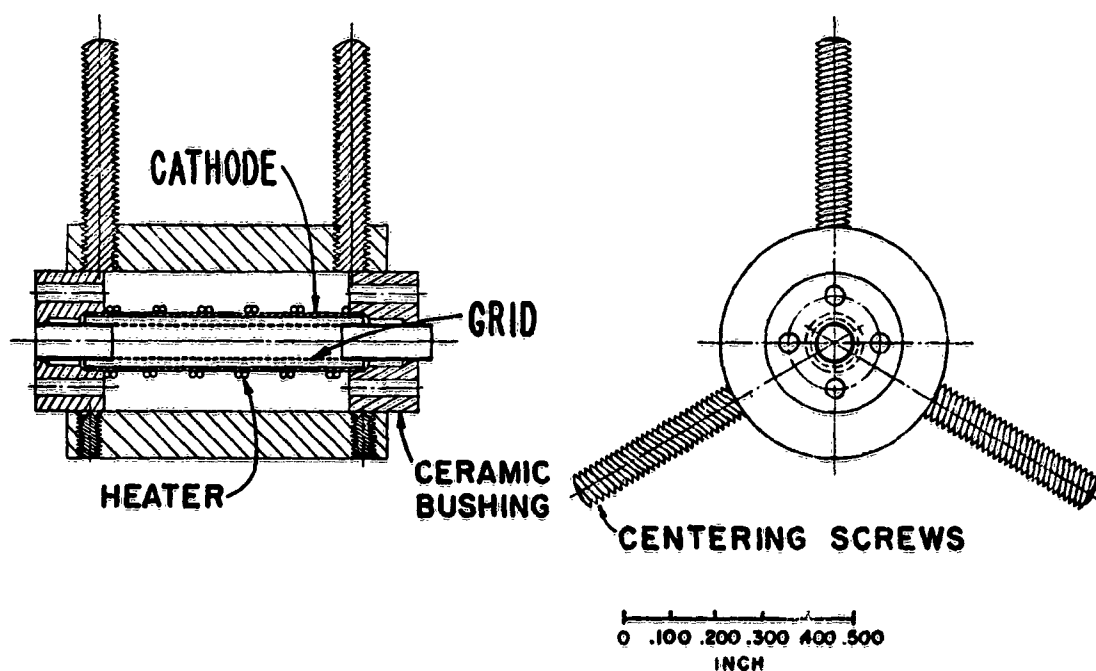
THE RECOMBINER

FIGURE 4

10

zero at some radius b. At this radius the space charge density is highest, falling off towards the axis where the potential becomes negative. Thus, the result of this arrangement is to achieve a relatively high density of electrons near the axis of the recombiner where the ion beam can readily be placed. A theoretical calculation for a similar parallel plane arrangement is given in Appendix I. The results of this calculation give a lower limit on the density that would be obtained in the cylindrical case. This limit certainly does not differ by more than a factor of 2 from the true cylindrical value.[38] If the accuracy of the remaining parts of the experiment becomes sufficiently high, more precise computations can be carried out.

The results of the computation have been used to plot the voltage distribution and the electron density for a typical case using the same dimensions as the recombiner. These are shown in Figures 5 and 6. As can be seen, the voltage and density vary rapidly with distance from the recombiner axis. Thus a proper average must be used to obtain the net density appropriate to the recombination. This is done by noting that the cross-section for recombination falls as approximately the inverse of the electron energy. Thus, the density at each point in the positive potential region of Figure 6 is divided by the ratio of the average energy at that point to the average energy at $V = 0$. The resulting modified density can then be averaged over the region of the recombiner occupied by the ion beam. When this is done for the case shown, the average density is found to be approximately $3 \times 10^9/cm^3$.

As is clear from the calculation of Appendix I, the current density passing through the grid must be known. This current density is readily found from the current intercepted by the grid if the grid transmission is known. It can be shown that if the grid-cathode spacing is much larger than the grid "hole" size, the electron transmission ratio through the grid is equal to the geometric grid transmission (ratio of "hole" area to total grid area). This is the case for the recombiner, and the grid transmission is 69%. The recombiner in this case is pulsed off by making the cathode positive with respect to the grid. The grid is held at ground potential so that the ion beam does not "see" the pulse.

The mechanical details of the recombiner are straightforward and can be seen in Figure 4. The grid is identical to the "nuvistor" grids employed in the RCA tube type of that name. The grid, which is self supporting, is allowed to slip in the ceramic bushings to prevent binding when the cathode is heated. The cathode is a nickel cylinder coated on the inside with a standard triple-oxide cathode coating. A uniform coating is achieved by rotating the cathode while the coating is being applied. The cathode heater is noninductive. Good activation of the recombiner cathode has been achieved, and current densities of the order of 100 ma/cm^2 have been passed through the grid.

The second method of achieving relatively high electron densities is based on the observation of Ash and Gabor[37] that the electron cloud inside a hollow cylindrical cathode is almost unavoidably neutralized by the presence of ions (probably barium) from the cathode. They find *fairly uniform* electron densities of the order of $10^{11}/cm^3$ in such hollow cylindrical cathodes. Since they discuss this matter at length and the work here on this approach has just started, nothing more will be said now about the magnitude and uniformity of the electron density. For the purposes of recombination measurements, however, the electron density in this "gridless" case can be modulated by the application of a magnetic field of the order of a hundred gauss applied parallel to the recombiner axis. The field would

11

RECOMBINER POTENTIAL
FOR: $J_o = 100$ MA/cm^2
$V_{GRID} = V_a = 50$ VOLTS

EXTRAPOLATED
PORTION

NON-THERMAL SOLUTION

$x = b$ (.0103 cm)

GRID LOCATED AT
$x = a$ (.085 cm)

V/VOLTS

X/cm

FIGURE 5

12

DISTANCE FROM CENTER OF RECOMBINER X/cm
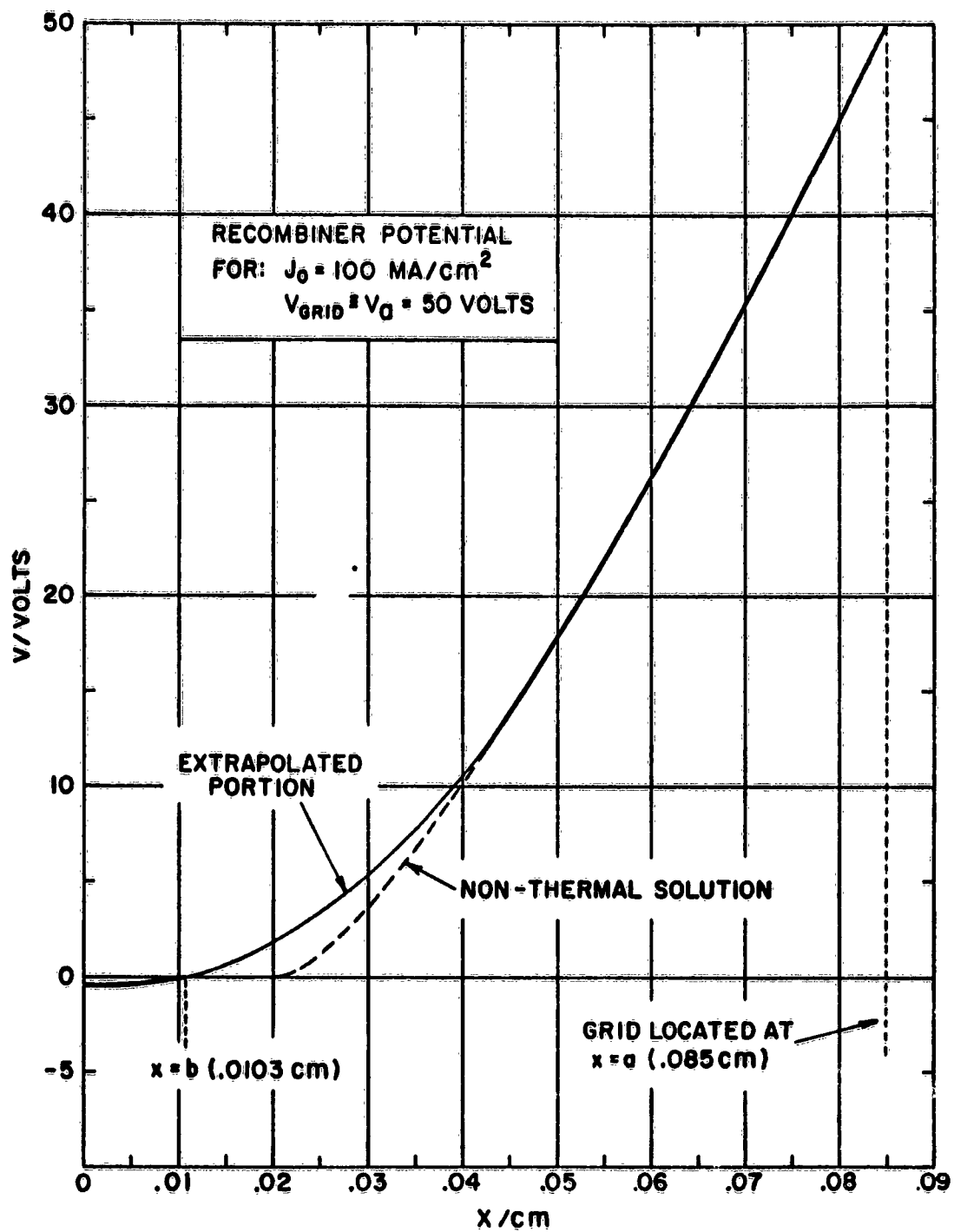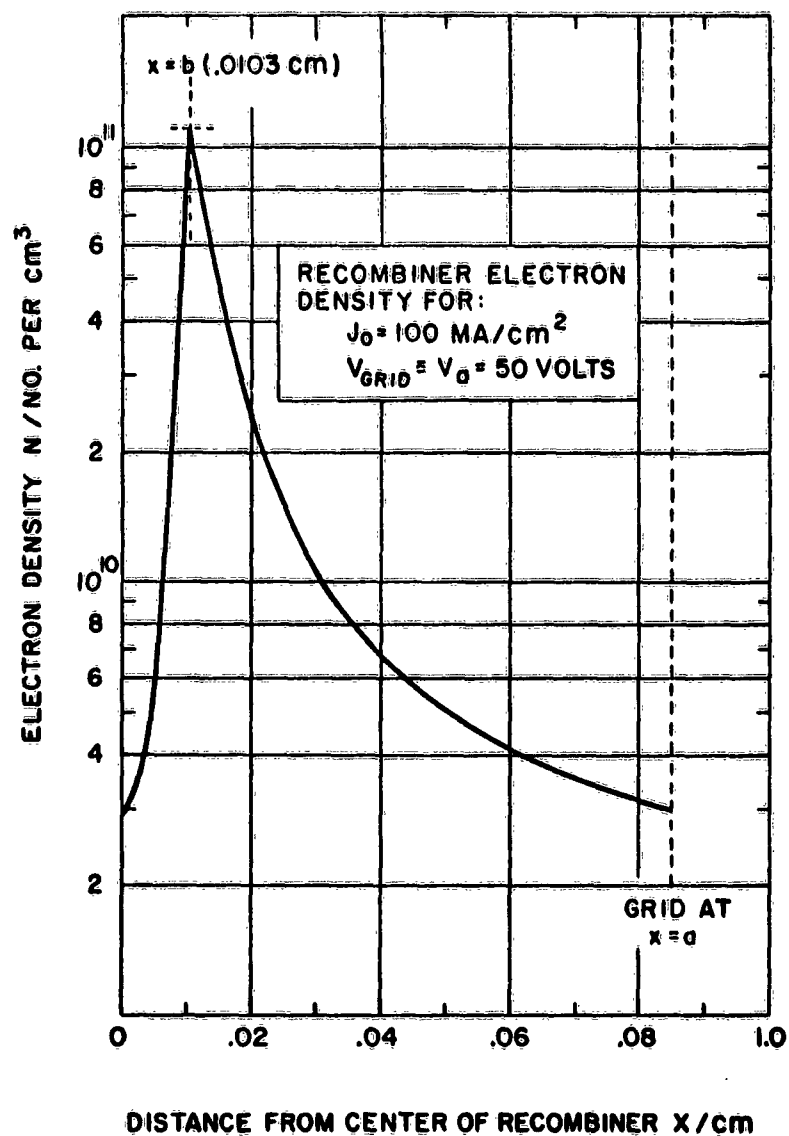
FIGURE 6

affect the ion beam only slightly while cutting off the electrons. (The electron orbit radius would be of the order of mills; the ion radius, ten feet.) The effect of the barium ions on the recombination has not yet been considered fully. It is thought initially that the main effect of these latter ions will be to scatter elastically some of the incoming cesium ions. Because of the wide acceptance angle of the neutral detector and the high rejection by the deflecting field of all charged ions, it seems that the recombination measurement will not be strongly affected. This is, of course, an initial and tentative conclusion.

13

ION DEFLECTOR AND FARADAY CAGE

The beam emerging from the recombiner is passed through a set of electric deflecting plates, which separate the ions from the atoms. A dc field across the plates deflects the ions to a Faraday cage, where the ion current is measured.

The geometry of the deflecting plates was optimized to cause 6 kv Cs-ions to deflect through an angle of 15° in a distance of one inch with a relatively low dc field value of 1500 volt/cm. The Faraday cage is a stainless steel cup, .79" long and .20" in diameter, supported by a single glass bead. Insulation is important here, as any leakage current would affect the reading of ion current. The secondary emission currents from the metal of the cage are suppressed by a small dc gradient applied between a suppressor plate and the cage.

Both the deflecting system and the Faraday cage operate satisfactorily.

14

THE ATOM DETECTOR

A survey was made of several possible methods for detecting low-density beams of neutral atoms possessing energies equivalent to a few kv. Among the methods considered were:

1. Detection of β-active Cs_{134} obtained by irradiation of the Cs_{133} beam with slow neutrons.

2. Use of a Faraday cage ion detector after reionization of the beam by electron bombardment.

3. Flashing of a tungsten surface previously coated by being exposed to the atom beam during a known period of time.

4. Direct contact ionization of the Cs-atoms at the surface of a heated metal, such as tungsten.

5. Use of a photomultiplier to detect and amplify the light signals produced by the impact of atoms in a scintillation crystal.

6. Production of secondary emission by bombarding a suitable surface with the atom beam, followed by electron multiplication.

After a preliminary study, methods 1 and 2 were rejected because the interaction processes involved have a cross-section too low to provide successful detection. Method 3 is essentially a dc version of method 4, without selective feature with respect to background Cs and foreign ions. Methods 4 and 5 were considered at length and are discussed in Appendices II and III. Method 6 was chosen as most promising for the experiment and is discussed below.

THE SECONDARY EMISSION DETECTOR AND ELECTRON MULTIPLIER

The secondary emission from metals has been used by a number of workers[39-42] to detect low-energy atomic beams. The values of y, the secondary emission coefficient, range from less than unity for low-energy beams up to values of over 20 for the impact of very fast Hg atoms on surfaces of sodium and potassium. In most cases, however, the value of y does not appear to be very sensitive to the nature of the solid surface but is markedly influenced by the presence of an absorbed gas layer. Work of Paetow and Walcher[43] with Cs^+ beams shows that, in cases where the surface has not initially been freed of all its absorbed oxygen, a composite film of Cs + O is formed and that a saturation value of y is reached when this composite film is one monolayer thick.

The secondary current caused by a neutral atom beam of the order of 10^{-15} amp, such as is expected in this experiment, can most conveniently be amplified with an electron multiplier. The first multiplier dynode is used as an atom-electron converter with conversion efficiency which appears to be of the order of unity for 6 kv cesium atoms. The remaining thirteen stages of the RCA C-7187J electron multiplier provide a current gain of up to 10^6, yielding an output current of 10^{-9} to 10^{-8} amp with a high signal-to-noise ratio.

Because the ratio of the multiplier output current to the input atom current is unknown and in addition is likely to vary with time because of surface contamination effects,

a means of calibration is essential. An approximate calibration can be made using ions rather than atoms. In this case the question of the charge dependence of the secondary electron detector must be raised. This dependence has been investigated by Barnett and Reynolds,[44] who report a response to neutral particles slightly larger than the response to the corresponding ions. The ratio varies between 1.37 and 1.62 for the few cases investigated. Due to the complicated nature of the secondary emission process and its dependence on the past history of the surface, it appears dangerous to generalize this result.

A promising method of calibration has been pointed out by Allison,[45] who notes that the question of charge dependence can be obviated by charge equilibrating the beam in either a gaseous charge exchange chamber or more simply in a thin metal foil just prior to the beam's impact with the secondary emitting surface. It is expected that this latter method will be employed here.

The "dark" current of electron multipliers is the sum of several contributing causes. The first is thermionic emission from the dynodes. Second, any residual ions accelerated back to the first dynodes cause the emission of pulses which will be fully amplified. Field emission from sharp points or edges at any electrode, and electrical ohmic and nonohmic leakage can play a roll but are usually less important on well designed multipliers.[46] The dc dark current output of electron multiplier type C-7187J was measured and found to range from .005 to .01 μA for applied voltages between 2500 and 3500 V.

An RCA Developmental Type C-7187J 14-stage Electron Multiplier cage with oxidized copper-beryllium dynodes was sealed to a vacuum flange and fixed at the neutral detector end of the instrument. The first dynode acts as an atom-electron converter. The remaining 13-stage system acts as an electron-multiplier which should provide a current gain of about 10^5 when the specified voltages are applied to the dynodes.

The secondary emission coefficient γ was obtained for Cs-ions of 6 kv energy by monitoring the ion current I_1 in the Faraday cup and measuring the secondary electron current I_2 at dynode 2. Results are tabulated below:

I_1 (μA)	I_2 (μA)	$\gamma = I_2/I_1$
.006	.012	2.00
.007	.0125	1.80
.010	.0275	2.75
.100	.300	3.00

Because of the perturbing effect of the stray field from the ion pump magnet, the multiplier gain was initially only 10^3. The gain was increased to its proper value of 10^5 by the expedient of bucking out the ion pump magnetic field with a small external magnet placed near the multiplier. Internal and external magnetic shields have been constructed, and will be adapted to the multiplier to correct for this perturbation.

It is intended to amplify the 100 cps modulated signal from the electron multiplier by a Tektronix type 122 preamplifier followed by a specially designed narrow-band amplifier previous to its detection in a phase-sensitive detector. The specially designed
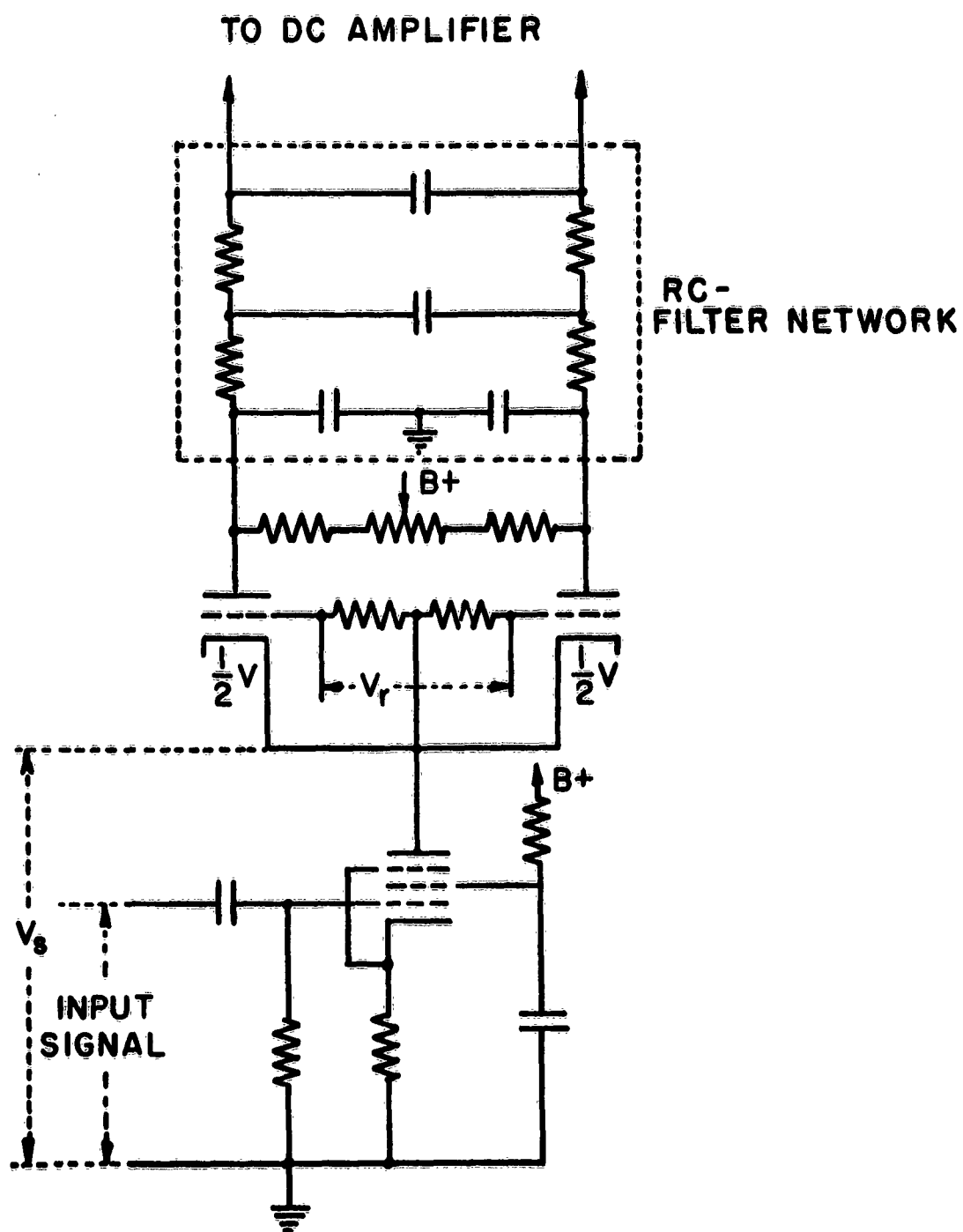
16

amplifier has 2 stages and uses a Twin-T network in a regenerative feedback loop. Figure 7 is a schematic of the amplifier and lock-in detector. The Twin-T filter is a high-Q three-terminal network with maximum impedance at its center frequency of 100 cps. The forward gain is 80. The feedback gain is variable from 0 to 180, resulting in a Q varying up to about 40 and in a bandwidth of 2.5 cps. The lock-in detector is an adaptation of a circuit devised by Shuster[47] for nuclear magnetic resonance measurements. Referring to Figure 8, a random incoming signal V_s applied at the cathodes of a dc-balanced twin-triode tube V leaves the dc-balance condition at the anodes unchanged. A reference signal V_r is taken from the modulating source and applied, out of phase, to the grids of the tube. V_r which is filtered out at the anodes by the long time constant of the RC network also leaves the dc-balance condition of the anodes unchanged. Only when the incoming signal has the same frequency and a fixed phase relationship to the reference signal will the steady balance condition at the anodes be disrupted. The lock-in detector thus provides a dc output voltage proportional to $V_s \cos \theta$ where θ is the phase shift between signal and reference input. The effective bandwidth, that is, the band from which noise is received, is half the reciprocal of the time constant of the filter network following the detector. Thus, $\Delta = \frac{1}{2RC}$. This time constant is adjustable from a few milliseconds to several seconds, resulting in an effective bandwidth as narrow as 0.1 cps. Additional gain is obtained by feeding the dc output voltage to a dc balanced voltmeter amplifier.

Both amplifier and lock-in detector are powered by a dc supply stabilized to 0.1% with respect to line fluctuations.

Tests of the Twin-T amplifier with sinusoidal input yielded the anticipated values of 80 for gain and of 2.5 cps for minimum bandwidth. The over-all voltage gain of the unit was about 140 for square wave input.

17

FIGURE 7. NARROW BAND AMPLIFIER AND LOCK-IN DETECTOR

18

TO DC AMPLIFIER

RC-
FILTER NETWORK

$\frac{1}{2}$V $\frac{1}{2}$V

V_r

B+

V_s

INPUT
SIGNAL

SCHEMATIC OF LOCK-IN DETECTOR
FIGURE 8

19

THE VACUUM ENCLOSURE AND PUMPING SYSTEM

As will be discussed shortly, it is essential to the success of this experiment that the lowest possible pressure be maintained in the experimental chamber. To this end, the system enclosure is constructed of mating flanged stainless steel sections which are sealed together with copper gaskets. Electrical connections are brought into the vacuum system through either ceramic or kovar-glass seals. The system is pumped by a Consolidated Vacuum Corporation 25-liter/sec ion-getter pump. The fore vacuum necessary to start the ion pump is obtained by use of a sorption fore pump. The entire apparatus can be baked at 400°C. As a result, the pumping system in no way contaminates the apparatus with organic or other undesired vapors and has maintained vacua of better than 2×10^{-9} mm Hg.

Mechanical alignment is provided by the enclosure through the accurate concentricity of the mating flanges. Thus, any subcomponent brought into alignment in an individual section will come into alignment with the remaining components automatically. This allows modifications to be incorporated into the apparatus with relative simplicity.

DISCUSSION

Having described the experimental method and apparatus in some detail, it is now appropriate to discuss the sensitivity of the method and what likelihood there is for the method to succeed.

Before entering into a discussion of the predicted sensitivity, the indications found from initial measurements will be described. Since these measurements were of an extremely limited nature and no calibrations were performed, they are mentioned only as a hopeful sign that the apparatus sensitivity may be sufficient to measure the desired cross-sections. The following was observed: with the ion beam focussed through the recombiner, the recombiner cathode hot, and the deflecting voltage adjusted so that the ions were collected in the ion collector, the dc current output of the electron multiplier increased by approximately one percent as the recombiner electrons were turned on by applying the appropriate voltage between grid and cathode. This effect was repeated statistically a number of times and can be explained either by the recombination of ions with the electrons or by an increase in pressure resulting in an increase in the atom current formed by exchange when the recombiner is on. Since the heater temperature is not varied when the electrons are turned on and since no pressure variation is observed, it seems likely that the effect is due to recombination. Unfortunately, further steps to identify the interaction could not be taken at that time because of the depletion of the ion source. As will be seen below, the size of the observed effect was not unreasonable. The question of a pressure variation occurring in the recombiner as the electrons are turned on and off arises from the fear that when the electrons are "on" the resulting electron bombardment of the grid will cause degassing to occur. In the "gridless" recombiner described earlier, this question will not arise. In the present system, the grid, being inside the cathode, is at cathode temperature. Prior to operation, both cathode and grid are heated to temperatures some 300°C higher than that normally used. Thus it is not unreasonable to hope that the grid will not degas when bombarded. Whether this is true or not will be checked in future experiments by turning "off" the electrons with a magnetic field without varying the grid cathode potential.

Although it is hoped that the question of apparatus sensitivity will be settled in a favorable way by our experimental activities in the near future, it is both useful and interesting to make a few predictions. It appears that the best available estimate of the size of the recombination coefficient is given by Hinnov and Hirschberg,[24] who verify a theory based on a three-body (two electrons and one ion) interaction with a spectroscopic investigation in helium and hydrogen plasmas. Converting their coefficients to cross-sections using equation (8), estimates of the size of the current of atoms due to recombination can be made as a function of the effective average electron density in the recombiner. The result of doing this is shown for an incoming ion current of 1 μA and an electron temperature such that $kT = 0.1$ eV (T = 1161°K) in the table below.

Assuming that a pressure of 10^{-8} mm Hg is maintained in the apparatus, the current due to exchange between the ions and the residual gas in the apparatus over the ion beam length between source and deflecting plates of 10 cm is calculated taking the exchange cross-section to be 10^{-16} cm^2. This neutral current due to exchange is 3.5×10^{-13} amps for an ion current of 10^{-6} amps. The measured dark current of the multiplier referred to the multiplier input is $10^{-8}/10^5 = 10^{-13}$ amps. Thus the spurious dc current at the multiplier

21

input is 4.5×10^{-13} amps. The signal due to recombination for electron densities in the range between 10^{10} and 5×10^{10} would be approximately one percent of the spurious dc current. Using the modulated system, the signal-to-noise power ratio may be calculated assuming full-shot noise is carried by both the signal current (I_R) and the spurious current (I_{sp}). The noise of the multiplier is accounted for by its contribution to the spurious current. Thus, the signal-to-noise ratio is

$$S/N = \frac{I_R^2}{2\,e\,(I_R + I_{sp})\,\Delta f} = \frac{I_R}{2\,e\,(1 + I_{sp}/I_R)\,\Delta f} .$$

Using this formula, the signal-to-noise power ratios shown in the table are found.

EXPECTED SIGNAL AND APPARATUS SENSITIVITY				
N_e electrons/cm^3	a From Ref. (24) sec^{-1}	$Q_R = a/\bar{v}$ cm^2	I_R Amps	S/N
10^9	1.69×10^{-12}	8.98×10^{-20}	8.98×10^{-17}	0.056
5×10^9	2.41×10^{-12}	1.28×10^{-19}	6.40×10^{-16}	2.80
10^{10}	3.29×10^{-12}	1.75×10^{-19}	1.75×10^{-15}	22.0
5×10^{10}	1.04×10^{-11}	5.53×10^{-19}	2.77×10^{-14}	5.0×10^3
10^{11}	1.92×10^{-11}	1.02×10^{-18}	1.02×10^{-13}	5.5×10^4

As can be seen from the table, if the recombination cross-sections are of the order of those shown, the signal-to-noise ratio will be of the order of unity or less at electron densities below 5×10^9. Clearly this is the minimum density that is permissible in order to get a measurement. If the cross-sections are a factor of 10 less than those assumed, a minimum electron density of 10^{10} is required. Under the conditions for which the initial measurements described at the beginning of this section were taken, it is likely that the electron space charge was at least partially neutralized. Thus the electron densities were probably in the 5×10^9 to 5×10^{10} range. The one-percent increase in output with the turning on of the recombiner is not inconsistent with these estimates.

CONCLUSION

The apparatus to implement the beam method of measuring recombination has been brought to a stage where initial measurements can be made. First measurements have given some indication that the method is sufficiently sensitive, although insufficient data were taken to estimate the cross-section. The work will continue while some of the improvements indicated for the ion gun and recombiner are being prepared.

APPENDIX I

CALCULATION OF POTENTIAL AND CHARGE DENSITY IN RECOMBINER

In the following refer to Figure 9. In an arrangement symmetric around the midplane, a current density of electrons (J_o) passes through each of the parallel plane grids which are separated by a distance $2a$ and maintained at a positive potential V_a with respect to the cathodes at zero potential. The cathode temperature is T. Assuming J_o to be sufficiently high while V_a is sufficiently low, the potential V between the grids is depressed to zero at $x = b$. Under these conditions, the potential in the center plane will be negative with value V_m. The region in which the potential is positive is denoted I, and where negative, II. Since current is introduced from both left and right, it can be shown that in Region I the density ρ is given by

$$\rho = - 2 \rho_o [1 - \operatorname{erf} \sqrt{eV/kT}] \tag{1}$$

while in Region II, by

$$\rho = - 2 \rho_o e^{eV/kT} . \tag{2}$$

Here

$$\rho_o = J_o \sqrt{m\pi/2\,kT} . \tag{3}$$

The resulting Poisson equations are

$$\text{Region I} \quad d^2V/dx^2 = 2\rho_o/\epsilon_o [1 - \operatorname{erf} \sqrt{eV/kT}]$$

$$\text{Region II} \quad d^2V/dx^2 = 2\rho_o/\epsilon_o\, e^{eV/kT} .$$

Letting $\alpha = e/kT$, the first integrals of these equations are

Region I

$$\left(\frac{dV}{dx}\right)^2 = \frac{4\rho_o}{\alpha\epsilon_o} \left[e^{\alpha V} (1 - \operatorname{erf} \sqrt{\alpha V}) + \frac{2}{\sqrt{\pi}} \sqrt{\alpha V} - e^{\alpha V_a} (1 - \operatorname{erf} \sqrt{\alpha V_a}) - \frac{2}{\sqrt{\pi}} \sqrt{\alpha V_a} \right]$$

$$+ (V_a')^2 \tag{4}$$

Region II

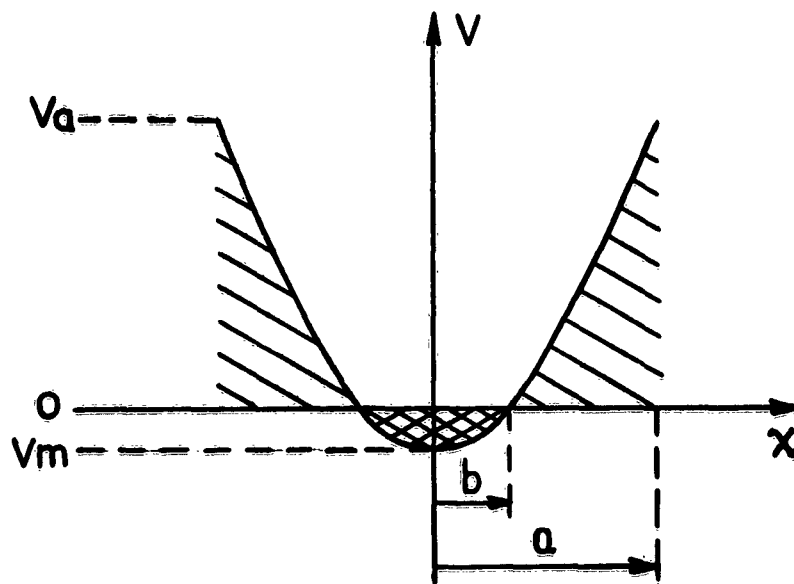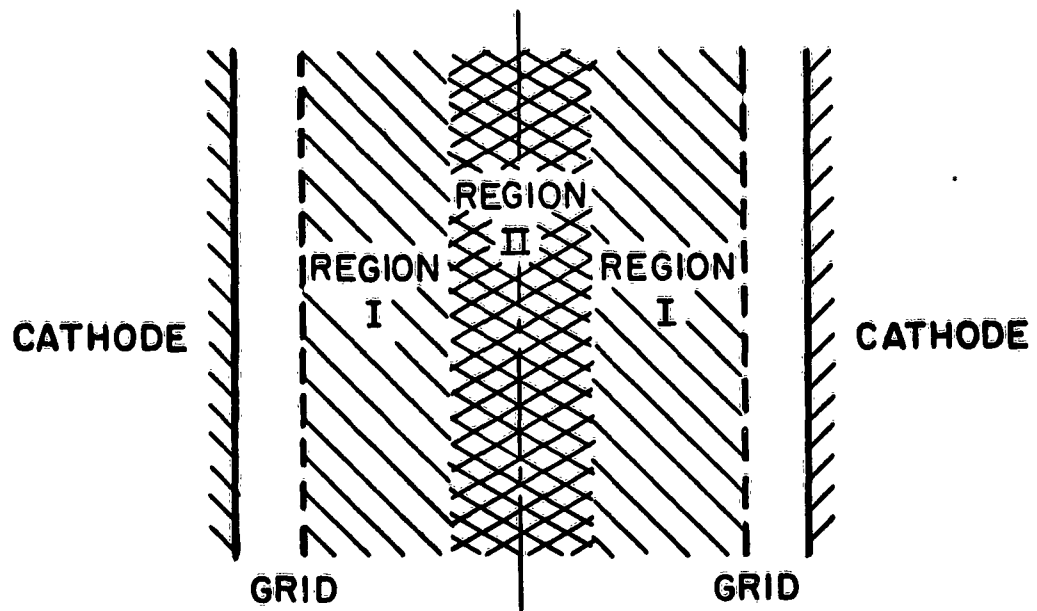$$\left(\frac{dV}{dx}\right)^2 = \frac{4\rho_o}{\alpha\epsilon_o} (e^{\alpha V} - e^{\alpha V_m}) . \tag{5}$$

24

DIAGRAM FOR RECOMBINER CALCULATION
FIGURE 9

If equation (4) is taken to the limit $T \to 0$, $a \to \infty$, the "nonthermal" equation results:

$$\left(\frac{dV}{dx}\right)^2 = \frac{8}{\epsilon_o} \sqrt{\frac{m}{2e}} \; J_o(\sqrt{V} - \sqrt{V_a}) + (V_a')^2.$$
(6)

In the following, use is made of the fact that both (5) and (6) can be integrated. Since equation (6) must hold for V sufficiently positive, the correct solution to equation (4) must pass smoothly into the solution of equation (6). At the same time, at x = b the field dV/dx must be continuous. Using these conditions, the solution in Region II and the nonthermal solution in Region I can be found. The solution for the remaining thermal part of Region I can then be found by a relatively short graphical extrapolation. Proceeding by this plan and matching (4) and (5) at x = b, V = 0, one gets

$$e^{aV_m} = \frac{2}{\sqrt{\pi}} \sqrt{aV_a} - \frac{\epsilon_o a}{4\rho_o} (V_a')^2 + e^{aV_a}(1 - \text{erf} \sqrt{aV_a}).$$
(7)

The potential V_a will be found below from the nonthermal solution. Integrating equation (5),

$$b - x = \left(\frac{\epsilon_o}{J_o a^{3/2}} \sqrt{\frac{2e}{m\pi}}\right)^{1/2} e^{-\frac{aV_m}{2}} \left[\sin^{-1}\sqrt{1 - e^{aV_m}} - \sin^{-1}\sqrt{1 - e^{a(V - V_m)}} \right]$$
(8)

and making the approximation that

$$\sin^{-1}\sqrt{1 - e^{aV_m}} \doteq \pi/2,$$

one obtains

$$e^{aV_m} \doteq \left[(\pi/2) \frac{\epsilon_o}{a\rho_o} \right] \frac{1}{b^2}.$$
(9)

For the nonthermal solution, the condition that dV/dx = 0 when V = 0 must hold. It then follows from (6) that

$$2/\sqrt{\pi} \sqrt{aV_a} - \frac{\epsilon_o a}{4\rho_o} (V_a')^2 = 0.$$

Thus (7) reduces to

$$e^{aV_m} = e^{aV_a}(1 - \text{erf} \sqrt{aV_a}),$$
(10)

26

where b is found from (9) and (3) in terms of e^{aV_m}:

$$b^2 = \frac{1}{e^{aV_m}} \left[\left(\frac{\pi}{2}\right)^2 \frac{\epsilon_0}{a J_0 \sqrt{\frac{\pi m a}{2e}}} \right] . \tag{11}$$

Thus, in Region II from (2) and (8) and using the same approximation as in (9) which implies that $x/b < .9$,

$$e^{aV} \doteq e^{aV_m}/\cos^2 (\pi x/2b) \tag{12}$$

$$\rho \doteq \rho_m/\cos^2 (\pi x/2b) \tag{13}$$

where

$$\rho_m = 2\rho_0 e^{aV_m} = \pi^2 \epsilon_0/a b^2 . \tag{14}$$

The value at x = b is found without approximation and is

$$\rho = 2\rho_0 .$$

In Region I, the solution of the nonthermal equation yields

$$V = \left(\frac{9}{2} \sqrt{\frac{m}{2e}} \frac{J_0}{\epsilon_0} \right)^{2/3} [x - (a - d)]^{4/3} \tag{15}$$

where $\quad d = V_a^{3/2} / (9/2 \sqrt{m/2e} \; J_0/\epsilon_0)^{1/2}$

and

$$\rho = 2 J_0 / \sqrt{2 eV/m} . \tag{16}$$

Thus, using (10) and (11) to find V_m and b, (12) and (13) give the solutions for the potential and density in Region II. The potential and density in the higher voltage part of Region I are given by (15) and (16), while the solution in the remainder of Region I can be found if desired by a graphical extrapolation.

As an illustration, the solutions for the case $J_0 = 100$ ma/cm^2, a = 0.85 cm and $V_a = 50$ volts have been plotted in Figures 5, 6. The complete nonthermal solution has been shown by the dotted portion on Figure 5 so that the extrapolated region is quite clearly defined.

Calibration

If a sufficient number of wall collisions are obtained prior to escape, the ionization efficiency can be made 100% and, neglecting noise, the neutral beam intensity can be taken as being equal to the ion current drawn from the detector.

Sputtering and Thermal Noise

Even high-purity tungsten, when heated, emits a number of ions, namely, K, Na, Rb, Ca and Al. Datz et al[52] have shown that this emission occurs as random pulses, a single pulse releasing as many as 10^6 ions in less than 100 μs. The average frequency of the pulses and the number of ions per pulse are temperature and pressure dependent. As a result of these considerations, the following noise estimates are made:

- Noise power due to sputtering: one 100 μsec square pulse per second of $.2 \times 10^{-6}$ ions results in zero-frequency Fourier components of 10^{-14} amp x sec and of 10^{-19} watts in a 10^9 Ω impedance. Assuming a 20 db attenuation at 100 cps, this amounts to 10^{-21} watt noise power

- Thermal noise (kT x bandwidth x gain) corresponding to 1200°K, a bandwidth of 1 cps, and a gain of 1, is 1.6×10^{-20} watt. The total noise power amounts to 1.7×10^{-20} watt.

A conservative figure of 10^{-15} A for the recombined beam intensity would result in a signal power of 10^{-21} watt and in a signal-to-noise-power ratio of 1:17. A more optimistic expectation of a signal 10^{-14} A would result in a signal power of 10^{-19} watt and in a signal-to-noise ratio of 6:1.

Thus it is clear that the surface ionization detecting system is rather marginal for this particular application. The following optimizing conditions will be essential:

a) Use of extremely pure tungsten as contact ionization surface.
b) Use of the smallest possible area of ionization surface.
c) The background pressure should be kept as low as possible.
d) The modulation frequency should be as high as possible, within the limits allowed to keep the input impedance of the preamplifier sufficiently high.

Practical Design

A surface ionization detector was designed based on these optimizing principles and is shown in Figure 10. The ionizing surface is high-purity tungsten (99.85% W, .08% 0, .05% Mo, .02%C). It is shaped as a cylindrical box with triangular base, providing, from the beam entrance aperture A, the desired multireflection path. Two ion-collecting plates C are fixed, one on top and the other at the bottom of the box. A noninductive heating element H is wound around the box, with a heat shield S_1. The detector is electrically shielded by box S_2.
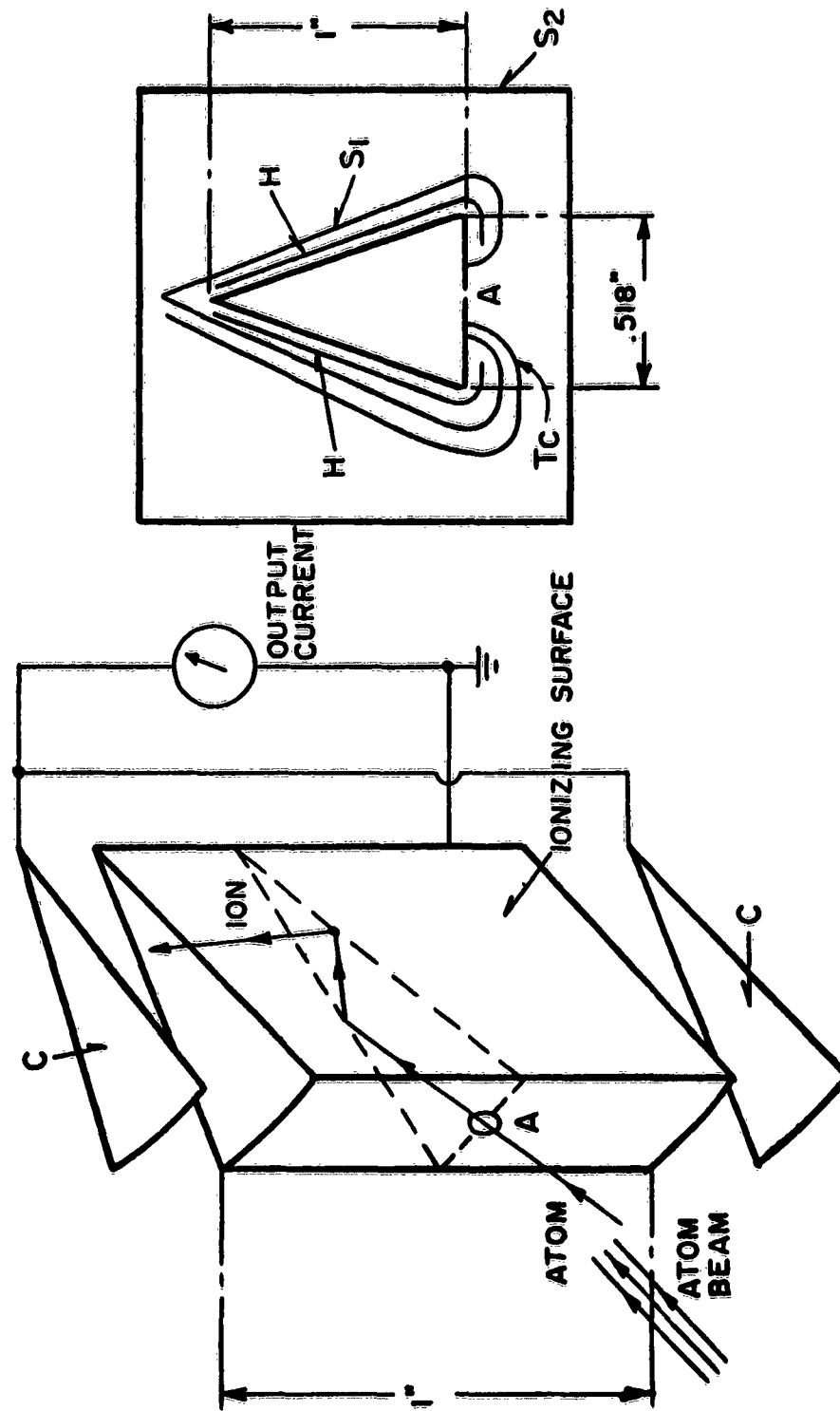
CONTACT IONIZING SURFACE

FIGURE 10

30

Preamplifier

A two-stage preamplifier (see Figure 11) was designed to match the very high output impedance of the detector to the lock-in amplifier-detector input impedance. The preamplifier uses a Victoreen Type 5800 electrometer tetrode dc-coupled to a Raytheon type CK6418 subminiature tetrode. The whole unit is mounted on the flange holding the stem of the detector. The box is made light-tight to minimize photoelectric grid currents, and airtight to minimize leakage in the input circuitry. The load-resistance of the detector is a Victoreen Hi-Meg Resistor of 10^{12} Ω, shunted by the 2 $\mu\mu$f input capacitance of the electrometer tube, resulting in an effective input impedance of 10^9 Ω at 100 cps. The voltage gain was found to be 25, and uniform over the frequency range of 5 to 2000 cps.
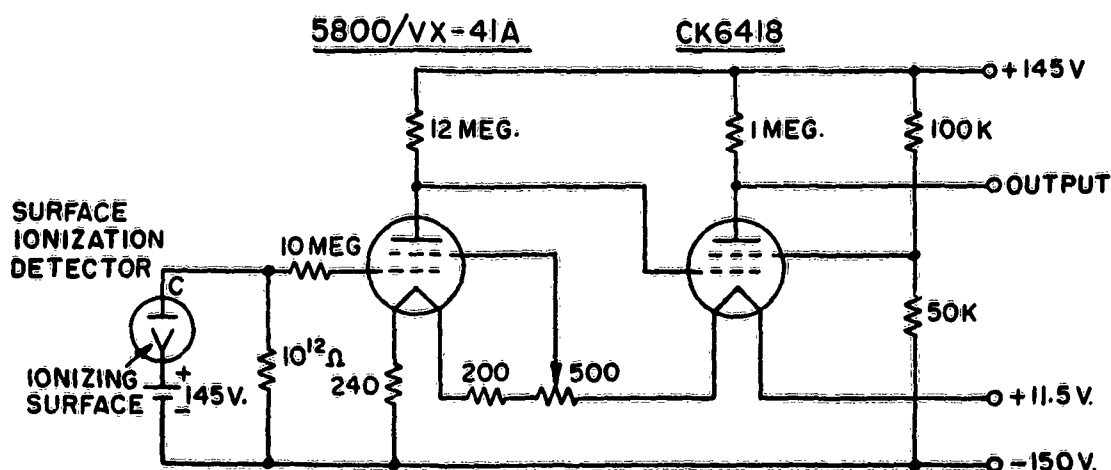
ELECTROMETER PREAMPLIFIER
FIGURE II

Tests

A leak developed in the stem, just prior to the tests of the detector. Because of this, and because more promising results were anticipated with the secondary-emission detector, further tests on this device have been postponed.

APPENDIX III

THE SCINTILLATION DETECTOR

Principle

During the course of study of ion exchange as a means of calibrating fast atom detectors, the possibility arose of using the light emitted when fast cesium atoms hit a thallium-activated Cs I crystal. This method has been used by Hall[53] and by several others[54,55] in their measurements of charge exchange equilibria of fast molecular H_2^+ beams.

The excitation of crystals by atom collision is a complex phenomenon involving Compton and photoelectric effects, as well as charge-exchange and other inelastic processes. In the low-energy region, the Compton-effect seems to predominate; and, due to their high mass number and hence high momentum value, even relatively low-energy Cs atoms are likely to cause excitation. The scintillator characteristics, its emission spectrum, its efficiency, and its decay time are determined by the molecular properties of its components, its impurity content, and its crystal structure.

An interesting feature of the excitation is that charge equilibrium of the beam is obtained as soon as the particle enters the crystal and that, as a consequence, the excitation is charge insensitive.[53] The same scintillation material can be used to measure the relative intensity of the neutral and of the charged beam components, with no change in response. A calibration chart established for ions should be valid for neutral atoms.

Another interesting feature of this detecting system is that, in association with proper electronic circuitry (pulse height discrimination), it leads itself to a display of the energy spectrum of the incident beam. As an example, using this technique and the coincidence detection technique, Sweetman[54] and Guidini[55,56] were able to isolate the four main processes involved in the dissociation of H_2^+ in collision with gases.

Only the scintillation crystal needs to be irradiated by the beam; the photomultiplier tube can be mounted outside the vacuum chamber, provided it is optically coupled to the crystal. This eliminates a variation in gain due to slow contamination of the dynodes by Cs deposit, or by oxygen when the system is assembled.

Sensitivity

In evaluating this detection method, several factors have to be considered with their effect on signal and noise: the scintillation material efficiency, the optical coupling between scintillator and photocathode, the photocathode radiant sensitivity, the dark current, and the multiplier gain.

Signal

A typical figure for the conversion efficiency of a CsI-Th crystal is the production of one photon of 5000A per 90 eV. Hence, a beam of 10^{-15}A of 6 kv Cs-atoms should

excite 4×10^5 photons per second, or a radiant power of .16 $\mu\mu$W at a wavelength of 5000A. Taking the optical coupling constant as 0.5, the power reaching the photocathode should amount to .08 $\mu\mu$W. With a value of over-all radiant sensitivity of 0.6 Amp/μW, such as is exhibited by RCA Type-7265 phototube, the original beam should result in a multiplier output amount of 5×10^{-8}A.

Dark Current

The equivalent dark-current input of the photomultiplier at room temperature is 2×10^{-10} lumen, resulting in an anode output current of 0.3×10^{-6}A. The equivalent noise input for a bandwidth of 1 cps is about 10^{-12} lumen, resulting in a noise output of current of 1.4×10^{-9}A.

Other Radiant Noise Sources

A good detection efficiency for Cs atoms demands a scintillation material with high density such as the alkali iodides, and their emission spectrum in turn (4200 to 5200A) dictates the choice of Type S-20 photocathode insofar as its spectral response is concerned. The vacuum chamber of the recombination apparatus now contains two light sources, the ion heater and the recombiner heater; both are oxide coated and heated to 1150-1200°K. Taking 0.5 as an average value for the emissivity of the oxides, the energy radiated at 4200 A, where type S-20 photocathode exhibits maximum sensitivity, is 10^{-7} of the maximum radiant energy of several watts emitted by the hot oxides at 25000A. Assuming an attenuation factor of 10 in the optical transmission path between heaters and photocathode, we are still left with 10^{-8} watts incident on a photocathode. This results in a prohibitive input signal to noise power ratio of $10^{-13}/10^{-8} = 10^{-5}$.

These considerations eliminate the possibility of using the scintillation detectors for the planned experiments.

33

BIBLIOGRAPHY

1. Hayner, L. J., "Über Stromverlauf and Lichtemission im Quecksilberbogen nach Ausschaltung der Spannung," *Zeitschrift Fur Physik*, Volume 35, January 9, 1926, pp. 365-386.

2. Kenty, C., "The Recombination of Argon Ions and Electrons," *Physical Review*, Volume 32, October 1928, pp. 624-635.

3. Mohler, F. L., "Recombination Spectra of Atomic Ions and Electrons," *Physical Review*, Volume 31, February 1928, pp. 187-194.

4. Mohler, F. L., "Recombination and Photo-Ionization," *Reviews of Modern Physics*, Volume 1, October 1929, pp. 216-227.

5. Boeckner, C. and Mohler, F. L., "Photo-Ionization of Caesium Vapor by Absorption Between the Series Lines," *Bureau of Standards Journal of Research*, Volume 5, October 1930, pp. 831-842.

6. Mohler, F. L., "Recombination of Ions in the Afterglow of a Cesium Discharge," *Bureau of Standards Journal of Research*, Volume 19, October 1937, pp. 447-456.

7. Mohler, F. L., "Recombination in the Afterglow of a Mercury Discharge," *Bureau of Standards Journal of Research*, Volume 19, November 1937, pp. 559-566.

8. Craggs, J. D. and Hopwood, W., "Electron-Ion Recombination in Hydrogen Spark Discharges," *Proceedings of the Physical Society*, Volume 59, September 1, 1947, pp. 771-781.

9. Biondi, M. A. and Brown, S. C., "Measurements of Ambipolar Diffusion in Helium," *Physical Review*, Volume 75, June 1, 1949, pp. 1700-1705.

10. Biondi, M. A. and Brown, S. C., "Measurement of Electron-Ion Recombination," *Physical Review*, Volume 76, December 1, 1949, pp. 1697-1700.

11. Holt, R. B., Richardson, J. M., Howland, B. and McClure, B. T., "Recombination Spectrum and Electron Density Measurements in Neon Afterglows," *Physical Review*, Volume 77, January 15, 1950, pp. 239-241.

12. Dandurand, P. and Holt, R. B., "Electron Removal in Mercury Afterglows," *Physical Review*, Volume 82, June 15, 1951, pp. 868-873.

13. Redfieled, A. and Holt, R. B., "Electron Removal in Argon Afterglows," *Physical Review*, Volume 82, June 15, 1951, pp. 874-876.

14. Richardson, J. M. and Holt, R. B., "Decay of the Hydrogen Discharge," *Physical Review*, Volume 81, January 1, 1951, pp. 153-154.

15. Biondi, M. A. and Holstein, T., "Concerning the Mechanism of Electron-Ion Recombination," *Physical Review*, Volume 82, June 15, 1951, pp. 962-963.

16. Stueckelberg, E. C. G. and Morse, P. M., "Computation of the Effective Cross Section for the Recombination of Electrons with Hydrogen Ions," *Physical Review*, Volume 36, July 1, 1930, pp. 16-23.

17. Bates, D. R., Buckingham, R. A., Massey, H. S. W. and Unwin, J. J., "Dissociation, Recombination and Attachment Processes in the Upper Atmosphere," *Proceedings of the Royal Society of London*, Volume 170, April 3, 1939, pp. 322-340.

18. Bates, D. R. and Massey, H. S. W., "Negative Ions of Atomic and Molecular Oxygen," *Philosophical Transactions of the Royal Society of London*, Volume 239, April 2, 1943, pp. 269-304.

19. Bates, D. R., "Dissociative Recombination," *Physical Review*, Volume 78, May 15, 1950, pp. 492-493.

20. Bates, D. R., "Electron Recombination in Helium," *Physical Review*, Volume 77, March 1, 1950, pp. 718-719.

21. Brown, S. C., "Basic Data of Plasma Physics," John Wiley and Sons, 1959, p. 195.

22. D'Angelo, N., "Recombination of Ions and Electrons," *Physical Review*, Volume 121, January 15, 1961, pp. 505-507.

23. Kuckes, A. F., Motley, R. W., Hinnov, E. and Hirschberg, J. G., "Recombination in a Heluim Plasma," *Physical Review Letters*, Volume 6, April 1, 1961, pp. 337-339.

24. Hinnov, E. and Hirschberg, J. G., "Electron-Ion Recombination in Dense Plasmas," *Physical Review*, Volume 125, February 1, 1962, pp. 795-801.

25. Bates, D. R. and Kingston, A. E., "Recombination through Electron-Electron Collisions," *Nature*, Volume 189, February 25, 1961, pp. 652-653.

26. McWhirter, R. W. P., "Rates of Recombination in Hydrogenic Plasmas," *Nature*, Volume 190, June 3, 1961, pp. 902-903.

27. Byron, S., Stabler, R. C. and Bortz, P. I., "Electron-Ion Recombination by Collisional and Radiative Processes," *Physical Review Letters*, Volume 8, May 1, 1962, pp. 376-379.

28. Johnson, E. D. and Malter, L., "A Floating Double Probe Method for Measurements in Gas Discharges," *Physical Review*, Volume 80, October 1, 1950, pp. 58-68.

29. Jeans, J., "*An Introduction to the Kinetic Theory of Gases,*" Cambridge, 1948, ·pp. 138-141, see equation 160. In Jean's notation

$\xi = C \sqrt{hm_2}$ where $h = 1/2kT$

$C = v_1 v_2 = N_o$ and $Q = \pi S_{12}^2$: or E. H. Kennard — *Kinetic Theory of Gases*. McGraw Hill, 1938, p. 107.

30. Massey, H. W. S. and Burhop, E. H. S., "*Electronic and Ionic Impact Phenomina,*" Oxford at the Clarendon Press, 1st edition, 1952, p. 619.

31. Ibid, p. 483.

32. Blewett, J. P. and Jones, E. J., "Filament Sources of Positive Ions," *Physical Review*, Volume 50, September 1, 1936, pp. 464-468.

33. Berghammer, J., Bloom, S., Eichenbaum, A. L. and Hammer, J. M., "Generation of 'Cool' Electrons for Low-Noise Microwave Tubes," Third Semi-Annual Report RCA Laboratories, Contract No. DA 36-039-sc-78151, March 15, 1960, pp. 4-7.

BIBLIOGRAPHY (Continued)

34. Spangenberg, K. R., *Vacuum Tubes*, McGraw-Hill, 1948, Chapter 13.

35. Pierce, J. R., *Theory and Design of Electron Beams*, D. Van Nostrand Co., New York, Second Edition 1954, p. 151, Pierce's Formula 9.17 if the numerics are not inserted becomes equation (10).

36. Smith, L. P. and Hartman, P. L., "The Formation and Maintenance of Electron and Ion Beams," *Journal of Applied Physics*, Volume 11, March 1940, pp. 220-229.

37. Ash, E. A. and Gabor D., "Experimental Investigations on Electron Interaction," *Proceedings of the Royal Society of London*, Volume 228, March 22, 1955, pp. 477-490.

38. Spangenberg, loc. cit, pp. 180-181.

39. Rostagni, C., "Untersuchungen Über Langsame Ionen and Neutralstrahlen," *Zeitschrift für Physik*, Volume 88, February 1921, p. 55.

40. Montagne, J. H., "Electron Loss Cross-Sections for Hydrogen Atoms Passing through Hydrogen Gas," *Physical Review*, Volume 81, March 15, 1951, p. 1026.

41. Stier, P. M., Barnett, C. F., Evans, G. E., "Charge States of Heavy-Ion Beams Passing through Gases," *Physical Review*, Volume 96, November 1954, p. 973.

42. Fedorenko, N. V., "Dissociation of the Molecular Ion H_2^+ in Collision with Gases," *Soviet Physics JETP*, Volume 36, August 1959, p. 267.

43. Paetow, H., Walcher, W., "Influence of Adsorption Layers Upon the Impact of Caesium Ions in Tungstem," *Zeitschrift für Physik*, Volume 110, 1938, p. 69.

44. Barnett, C. F., Reynolds, H. K., "Charge Exchange Cross-Sections of Hydrogen Particles in Gases at High Energies," *Physical Review*, Volume 109, January 1958, p. 355.

45. Allison, S. K., "Experimental Results on Charge Changing Collisions of Hydrogen Atoms and Ions at Kinetic Energies above 0.2 kev," *Review of Modern Physics*, Volume 30, October 1958, p. 1137.

46. Morton, G. A., "Photo-multipliers for Scintillation Counting," *RCA Review*, Volume 10, December 1949, p. 525.

47. Schuster, N. A., "A Phase-Sensitive Detector Circuit Having High Balance Stability," *Review of Scientific Instruments*, Volume 22, April 1951, p. 254.

48. Langmuir, I., Kingdom, K. H., "Thermionic Effects Caused by Vapours of Alkali Metals," *Proceedings of the Royal Society*, Series A, Volume 107, January 1, 1925, p. 61.

49. Taylor, J. B., Langmuir, I., "The Evaporation of Atoms, Ions and Electrons from Caesium Films on Tungsten," *Physical Review*, Volume 44, September 1933, p. 423.

50. Copley, M. J., Phipps, T. E., "The Surface Ionization of Potassium on Tungstenu, *Physical Review*, Volume 48, December 1935, p. 960.

BIBLIOGRAPHY (Continued)

51. Datz, S., Taylor, E. H., "Ionization on Platimum and Tungsten Surfaces — I.
The Alkali Metals," *Journal of Chemical Physics*, Volume 25, September 1956, p. 389.

52. Minturn, R. E., Datz, S., Taylor, E. H., "Thermal Emission of Alkali Ion Pulses from
Clean and Oxygenated Tungsten," *Journal of Applied Physics*, Volume 31, May 1960,
p. 876.

53. Hall, Th., "Ratio of Cross-Sections for Electron Capture and Electron Loss by Proton
Beams in Metals," *Physical Review*, Volume 79, August 1950, p. 504.

54. Sweetman, D. R., "Dissociation of H_2^+ Ions by Hydrogen," *Physical Review Letters*,
Volume 3, November 1, 1959, p. 425.

55. Guidini, J., Belna, R., Briffod, G. and Manus, C., "Etude des réactions produites
par des ions moléculaires d'hydrogène traversant un gaz," *Compte Rendus*, Volume
251, November 28, 1960, p. 2496.

56. Guidini, J., "Etude des réactions produites par un faisceau d'ions moléculaires
traversant des gaz d'hydrogène et d'hélium neutres," *Compte Rendus*, Volume 252,
May 1961, p. 2848.

DISTRIBUTION LIST

No. of Copies

Ofc of Ord, ODDR&E	2
First US Army	1
Fourth US Army	1
Sixth US Army	1
USACGSC	1
USAARMBD	1
USAAVNBD	1
USATMC (FTZAT), ATO	1
USAPRDC	1
DCSLOG	1
Rsch Anal Corp	1
ARO, Durham	2
Ofc of Maint Engr, ODDR&E, OSD	1
NATC	1
ARO, OCRD	1
CRD, Earth Scn Div	1
USAERDL	2
USAOTAC, Center Line	4
OrdBd	1
QM Comb Dev Ag	1
QMRECOMD	1
QMFEA	1
QMFSA	1
SigBd	2
USATCDG	1
USATB	1
USATMC	20
USATSCH	4
USATRECOM	24
USATTCA	1
USATTCP	1
OUSARMA	1
USATRECOM LO, USARDG (EUR)	1
USAEWES	3
C CO, 721st Trans Bn (Ry Opr)	1
B Co, 721st Trans Bn (Ry Opr)	2
USATDS	2
USARPAC	1
USARHAW	2
ALFSEE	1
USACOMZEUR	3
APGC (PGAPI)	1
Air Univ Lib	1

No. of Copies

ASD (ASRMPT)	1
CNO	1
CNR	3
BUWEPS, DN	4
ACRD(OW), DN	1
USNCEL	1
USNSRDF	1
BUY&D, DN	1
USNPGSCH	1
Dav Tay Mod Bas	1
MCLFDC	1
MCEC	1
USCG	1
NAFEC	3
Langley Rsch Cen, NASA	2
MSC, NASA	1
NASA, Wash., D. C.	6
Ames Rsch Cen, NASA	2
Lewis Rsch Cen, NASA	1
Sci & Tech Info Fac	1
USGPO	1
ASTIA	10
USAMRDC	1
USAMRL	1
HUMRRO	2
CIA	1
RCA	10
USSTRICOM	1
MOCOM	3

AD _____ Accession No. _____

Radio Corporation of America, Princeton, N. J.
RESEARCH ON THE VOLUME RECOMBINA-
TION OF CESIUM IONS — P. V. Goedertier
and J. M. Hammer

Interim Engineering Report No. 1, October 15,
1962 — 41 pp. illus. – tables
(Contract DA44-177-TC-694) Task 9R99-20-991-08
TCREC 62-82 — Unclassified Report

An apparatus to implement a new method of meas-
uring radiative recombination based on the pas-
sage of an ion beam through an electron cloud has
been constructed. Initial tests of the sub-compo-
nents and of the apparatus itself give some indi-
cation that the method will work. The method and
the apparatus are described in detail and the im-
plications of the initial measurements are dis-
cussed.

AD _____ Accession No. _____

Radio Corporation of America, Princeton, N. J.
RESEARCH ON THE VOLUME RECOMBINA-
TION OF CESIUM IONS — P. V. Goedertier
and J. M. Hammer

Interim Engineering Report No. 1, October 15,
1962 — 41 pp. illus. – tables
(Contract DA44-177-TC-694) Task 9R99-20-991-08
TCREC 62-82 — Unclassified Report

An apparatus to implement a new method of meas-
uring radiative recombination based on the pas-
sage of an ion beam through an electron cloud has
been constructed. Initial tests of the sub-compo-
nents and of the apparatus itself give some indi-
cation that the method will work. The method and
the apparatus are described in detail and the im-
plications of the initial measurements are dis-
cussed.

AD _____ Accession No. _____

Radio Corporation of America, Princeton, N. J.
RESEARCH ON THE VOLUME RECOMBINA-
TION OF CESIUM IONS — P. V. Goedertier
and J. M. Hammer

Interim Engineering Report No. 1, October 15,
1962 — 41 pp. illus. – tables
(Contract DA44-177-TC-694) Task 9R99-20-991-08
TCREC 62-82 — Unclassified Report

An apparatus to implement a new method of meas-
uring radiative recombination based on the pas-
sage of an ion beam through an electron cloud has
been constructed. Initial tests of the sub-compo-
nents and of the apparatus itself give some indi-
cation that the method will work. The method and
the apparatus are described in detail and the im-
plications of the initial measurements are dis-
cussed.

AD _____ Accession No. _____

Radio Corporation of America, Princeton, N. J.
RESEARCH ON THE VOLUME RECOMBINA-
TION OF CESIUM IONS — P. V. Goedertier
and J. M. Hammer

Interim Engineering Report No. 1, October 15,
1962 — 41 pp. illus. – tables
(Contract DA44-177-TC-694) Task 9R99-20-991-08
TCREC 62-82 — Unclassified Report

An apparatus to implement a new method of meas-
uring radiative recombination based on the pas-
sage of an ion beam through an electron cloud has
been constructed. Initial tests of the sub-compo-
nents and of the apparatus itself give some indi-
cation that the method will work. The method and
the apparatus are described in detail and the im-
plications of the initial measurements are dis-
cussed.